Desalination and Water Treatment
www.deswater.com

doi: 10.5004/dwt.2021.27030

221 (2021) 291–302
May

Synergistic degradation of triclosan from aqueous solution by combination of sulfate radical and electrocoagulation process

Arezo Rezaie[a,b], Mohammad Taghi Ghaneian[a,*], Ali Fatehizadeh[c,d], Fahimeh Teimouri[a], Mohammad Mehdi Amin[c,d]

[a]*Environmental Science and Technology Research Center, Department of Environmental Health Engineering, School of Public Health, Shahid Sadoughi University of Medical Sciences, Yazd, Iran, email: mtghaneian@gmail.com (M.T. Ghaneian), arezorezaie373@gmail.com (A. Rezaie), f.teimori62@gmail.com (F.Teimouri).*
[b]*Student Research Committee, Shahid Sadoughi University of Medical Sciences, Yazd, Iran*
[c]*Department of Environmental Health Engineering, School of Health, Isfahan University of Medical Sciences, Isfahan, Iran, emails: a.fatehizadeh@hlth.mui.ac.ir (A. Fatehizadeh), amin@hlth.mui.ac.ir (M.M. Amin)*
[d]*Environment Research Center, Research Institute for Primordial Prevention of Non-Communicable Disease, Isfahan University of Medical Sciences, Isfahan, Iran*

Received 12 September 2020; Accepted 13 January 2021

ABSTRACT

The triclosan (TC) is classified as antibacterial compound as an emerging pollutant, which is extensively used in pharmaceuticals and personal care products. The present study evaluated the degradation efficiency of TC by combination of persulfate radical and electrocoagulation (PS-EC) process from synthetic industrial wastewater. To obtain optimum condition, the effect of influencing parameter on PS-EC process including solution pH, reaction time, current density, PS dose, concentration of electrolyte, initial concentration of TC, and electrode arrangement were systematically investigated. The increase of the current densities from 0.67 to 2.71 mA/cm^2 resulted in an increase of TC degradation efficiency from 58.7% to 65.9% after 35 min of reaction time. Up to 99.5% of TC was degraded by PS-EC process after 35 min reaction time at optimum condition including PS dose: 250 mg/L, current density: 2.71 mA/cm^2, electrolyte concentration: 2.5 g/L, and solution pH: 7. The operating cost including electrode and energy was calculated as 164,782 $Rial/m^3$. The Brunauer–Emmett–Teller analysis of produced sludge during PS-EC process indicated that the specific surface area, total pore volume, and mean pore diameter were 97.8 m^2/g, 0.19 cm^3/g, and 7.8 nm, respectively.

Keywords: Electrocoagulation; Sulfate radical; Persulfate anions; Triclosan

1. Introduction

The pharmaceutical and personal care products (PPCPs), as an emerging pollutant, with potential toxicity and oxidation resistance characteristics have attracted considerable attention and are widely consumed for human and animal health worldwide [1,2]. Among PPCPs, the triclosan (5-chloro-2-(2,4-dichlorophenoxy)-phenol) (TC) is an antibacterial agent and have variety of applications including shampoos, detergents, toothpaste, and lotions. In addition, TC is used as an additive in many industries such as textile, plastic, and polymer [1,3,4]. Due to extensive application of TC, it was detected in various environments, including groundwater, river water, sediments, and biota, which

---

* Corresponding author.

depicts the adverse effect on ecosystems [5]. The EPA has designated TC as a processor in dioxins formation and tends to accumulate in adipose tissue of humans and animals [6]. During disinfection of drinking water, the TC can react with chlorine and to produce chloroform or chlorinated phenols such as 2-4-dichlorophenol (2,4-dichlorophenol and 2-4 produce 6-trichlorophenol (2,4-trichlorophenol) as possible carcinogen compounds [6,7].

Because of extensive discharge of TC into wastewater, it is important to develop an efficient strategy for water and wastewater treatment [8]. The various treatment methods were adopted to destroy and remove TC including conductive diamond electrochemical-oxidation, conductive-diamond sono-electrochemical oxidation, ozonation, magnetic activated carbon [9–12]. The main drawback of mentioned process is low efficiency due to low concentrations of pollutants that control the electrolysis of organic waste with mass transfer rate [11], economic considerations for full-scale implementation [13], limited porosity and low surface area of char [12], which attempts have been made to find the efficient treating methods. According to the literature [14], ozone has been shown to be very effective in TC oxidation and ultimately eliminating its antibacterial activity. Ozone appears to be an effective tool for killing TC antibacterial activity during wastewater treatment. Besides, Jiang et al. [15] confirmed the effect of $KMnO_4$ on the removal of oxidative TC in natural water and wastewater.

Nowadays, the advanced oxidation processes (AOPs) have been commonly used for organic compounds elimination, due to their advantages, such as easy operation, high efficiency, and low cost [16]. The restricted standards of environmental and variety of constraints lead to high attention on the application of the AOPs based on the sulfate radical ($SO_4^{\bullet-}$) as a strong oxidation agent for wastewater treatment and in situ chemical oxidation [17,18]. The $SO_4^{\bullet-}$ radical has higher redox potential (2.5–3.1 V) than hydroxyl ($^{\bullet}OH$) radicals (1.8–2.7 V) and is highly selective [16,19]. Besides, the $SO_4^{\bullet-}$ radicals have a longer half-life ($t_{1/2}$: 30–40 μs) than $^{\bullet}OH$ radicals ($t_{1/2}$: 1 μs), which leads to highest mass transfer and complete contact between the radicals and the organic pollutant [2]. The persulfate anions ($S_2O_8^{2-}$) (redox potential: 2.01 V) are stable and strong chemical oxidizers that might be activated by various methods to form $SO_4^{\bullet-}$ radicals [20]. In addition, the advantages of persulfate anion (PS) are including low cost, high solubility, high stability of its radical in various conditions, solid form, and ease of handling [21]. The activation methods of PS are including application of heat [22], ultraviolet (UV) light [22], transition metal, ultrasonic irradiation, alkaline conditions, electrical current and their combination as illustrated in Eqs. (1)–(4) [23–26].

$$S_2O_8^{2-} \xrightarrow{\text{Heat}} 2SO_4^{\bullet-} \tag{1}$$

$$S_2O_8^{2-} \xrightarrow{\text{hv}} 2SO_4^{\bullet-} \tag{2}$$

$$S_2O_8^{2-} + M^{n+} \longrightarrow SO_4^{\bullet-} + M^{(n+1)} + SO_4^{2-} \tag{3}$$

$$S_2O_8^{2-} \xrightarrow{\text{Ultrasonic wave}} 2SO_4^{\bullet-} \tag{4}$$

Among the transition metals, ferrous iron salts (Fe^{2+}) are mostly used to activate PS with an activation energy of 50.23 kJ mol⁻¹ (Eq. (5)).

$$S_2O_8^{2-} + Fe^{2+} \longrightarrow SO_4^{\bullet-} + Fe^{3+} + SO_4^{2} \tag{5}$$

When Fe^{2+} salts were used as PS activator, consumption of large amounts of iron, production of high volume of sludge, need for high dose of Fe^{2+} to activate persulfate due to difficulty in producing Fe^{2+} after conversion to Fe^{3+}, and in case of excessive presence of divalent iron, iron reacts with sulfate radicals and acts as a scavenger and reduces efficiency; these are the disadvantages of this method [24]. To overcome the mentioned drawbacks, attempts have been made to use electrocoagulation process as an environmental friendly technology for efficient treatment of various industrial wastewaters [27]. In fact, this process is the destabilization of suspended, emulsified, or soluble pollutants in the aqueous medium by introducing an electric current into the environment. The electrocoagulation process is the electrochemical production of metal ions (such as Al and Fe) that act as destabilizing agents and neutralize the electrical charge to remove contaminants [28]. Its advantages include economic efficiency with simple equipment and easy operation, short working time, small or insignificant amount of chemicals and sludge reduction [29].

In recent years, the continuous Fe^{2+} production by applying electric current on the iron electrodes has been proposed as a new alternative method for PS activation according to Eqs. (6) and (7).

$$Fe_{(s)} \longrightarrow Fe^{2+} + e^{-} \tag{6}$$

$$Fe^{3+} + e^{-} \longrightarrow Fe^{2+} \tag{7}$$

In this process, after separation of Fe^{2+} from the anode electrode, the Fe^{2+} reacts with PS anions to generate $SO_4^{\bullet-}$ radicals (Eq. (5)) and gets converted to Fe^{3+} cations and after that, Fe^{3+} is regenerated in the cathode to Fe^{2+} and as a consequence, iron consumption and sludge production minimized [30]. Therefore, the electrolysis of PS anions to generate $SO_4^{\bullet-}$ radicals may have a strong influence on the oxidation and degradation of pollutants from wastewater by the electrochemical process [31].

Song et al. [32] performed the electrochemical activation of PS in the boron-doped diamond (BDD) anode, which resulted in high efficiency in the electrochemical activation of PS and also Bu et al. [33] activated PS anions by direct electric current using using BDD anode and reported that high degradation of atrazine obtained and activation of PS led to significant reduction of electrolyte demand.

However, to the best of our knowledge from reviewing the literature, no report is available to date on the degradation of TC from wastewater by PS-EC process. Accordingly, the present work was a laboratory scale study and evaluated the effectiveness of operation parameters including solution pH, current density, reaction time, PS dose, concentration of electrolyte, initial concentration of TC, and electrode arrangement on degradation efficiency of TC by

PS-EC process. In addition, the kinetics of TC degradation was evaluated. Finally, in order to characterize the properties of produced sludge, Fourier-transform infrared (FTIR) spectroscopy, X-ray diffraction (XRD), scanning electron microscopy (SEM), Brunauer–Emmett–Teller (BET), and energy-dispersive X-ray spectroscopy (EDS) were employed.

2. Materials and methods

2.1. Chemicals and reagents

All the chemicals used in this study include TC, sodium persulfate ($Na_2S_2O_8$, CAS #: 7775-27-1), and sodium chloride (NaCl, CAS #: 7647-14-5) were analytical grade and bought from Merck Co. (Germany). All the working solutions were prepared by dissolution of mentioned chemicals in the distilled water. The main characteristics of TC are summarized in Table 1.

2.2. Setup of PS-EC process and procedure

The PS-EC process was made from plexiglass with total volume of 1,000 mL and working volume of 500 mL and equipped with two pair of iron and aluminum sheets as an anode and cathode electrodes (16 cm × 6 cm × 2 mm). During experiments, the electrodes were vertically immersed in the treating solution and providing 147.2 cm^2 of active surface of electrodes. The distance between the paired anode and cathode was maintained constant and taken to be 2 cm. The pair of electrodes with monopolar arrangement was connected to a DC power supply (DAZHENG PS-305D, China), which is capable of supplying the highest electrical potential and current of 30 V and 5 A, respectively. For batch experiments of TC degradation by PS-EC process, 500 mL of the synthetic wastewater containing a prespecified concentration of TC was transferred into the reactor equipped with the previously described electrodes; the density of the electrical current was regulated at the desired value, the electrical current was established between electrodes, and the reaction was started and allowed to continue up to the specified time. In order to ensure well mixing of reactor content and solution pH adjustment, the magnetic stirrer at mixing intensity of 500 rpm and HCl and NaOH (0.1 M) was used. After desired reaction time, the suspension was centrifuged at 3,000 rpm for 5 min and then analyzed for residual concentration of TC cyanide. At the beginning of each experiments, the pair of electrodes was cleaned with 15% HCl and then extensively rinsed with distilled water. All batch experiments of TC degradation by PS-EC process were performed at ambient temperature by using NaCl as electrolyte. The applied conditions of each experiment are summarized in Table 2.

2.3. Analysis

The residual concentration of TC after each experiment was quantified with high performance liquid chromatography (HPLC, Waters, model No. 486) equipped with UV detector (203 nm) and C18 packed column (Nucleosil® 5 µm C18 100 A, LC Column 250 × 4.6 mm, Ea). The mobile phase was made by acetonitrile and water (volumetric ratio of 75:25) at flow rate of 1 ml/min [34].

In order to determine the characteristics of produced sludge during experiments, at first, the collected sludge was dried for 24 h at 105°C. Then, the dried sludge sample was subjected to SEM observation (TESCAN, MIRA III, Czech Republic), XRD (PHILIPS, PW1730, The Netherlands), EDS (FESEM, TESCAN, Czech Republic), FTIR (Thermo, Avatar, United States), and BET (BEL, BELSORP MINI II, Japan) analysis.

2.4. Operating cost

The main components of operating costs are energy and electrode costs, which are calculated using Eq. (8).

Table 1
Main characteristics of TC

Properties	Description
Molecular structure	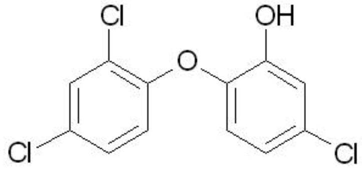
Chemical formula	$C_{12}H_7Cl_3O_2$
Molar mass (g/mol)	289.54
Boiling point	120°C
CAS Number	3380-34-5
Density (g/cm^3)	1.49

Table 2
Experimental conditions employed in TC degradation by PS-EC process

Studied parameter	Experimental condition					
	pH	Reaction time (min)	Current density (mA/cm^2)	PS dose (mg/L)	NaCl (g/L)	TC conc. (mg/L)
Solution pH	3–9	30	1.35	100	1	20
Reaction time	7	5–90	1.35	100	1	20
Current density	7	35	0.67–3.39	100	1	20
PS dose	7	35	2.71	100–300	1	20
Electrolyte concentration	7	35	2.71	250	1–3	20
Initial TC concentration	7	35	2.71	250	2.5	20–120

$$\text{Operation cost} = C_{\text{energy}} + C_{\text{electrode}} \tag{8}$$

In the above equation, C_{energy} and $C_{\text{electrode}}$, respectively, are the energy consumption and the electrode per cubic meter of water [35].

The electrode and energy consumption in EC process were calculated by using Eqs. (9) and (10).

$$\text{Energy consumption} = \frac{VIt}{v} \tag{9}$$

$$\text{Electrode consumption} = \frac{ItM}{zFv} \tag{10}$$

where V is applied voltage (V), I is current (A), t is EC time(s), v is volume of treated wastewater (m^3), F is Faraday's constant, M_w is molar mass of iron and aluminium and z is the number of electron transfer [36].

3. Result and discussion

3.1. Effect of solution pH

To investigate the effects of solution pH on TC degradation by PS-EC process, the experiments were performed with different solution pH ranging from 3.0 to 9.0 at initial TC concentration of 20 mg/L with 30 min reaction time. The variations of TC degradation efficiency as a function of solution pH are shown in Fig. 1.

As depicted, the degradation efficiency of TC improved from 61.4% to 68.5% with increasing pH of the solution from 3 to 7. After that, the TC degradation efficiency promptly declined and reached to 26.3% at solution pH of 9. The highest degradation efficiency of TC (68.5%) was obtained at solution pH of 7 and selected as optimum solution pH for the rest of experiments.

In the electrochemical processes, in which Fe^{2+} is used to activate PS anion and generate $SO_4^{\bullet-}$ radical, the pH of the solution affects on the species and state of iron in the solution, as well as the reaction rate of the $SO_4^{\bullet-}$ radical with organic pollutant [37]. With gradually increasing the pH from acidic conditions to basic range, most of the iron present in the system alters from Fe^{2+} to Fe^{3+} state; since only Fe^{2+} is capable to activate PS anions, the degradation efficiency of process significantly reduced with Fe^{2+}/Fe^{3+} ratio decreasing [38]. Furthermore, under acidic conditions, the $HS_2O_8^{2-}$ and SO_4^{2-} are predominant ions compared with PS anions and lead to minimizing the $SO_4^{\bullet-}$ radical generation [39]. At solution pH lower than 4, the Fe^{3+} complexes formation resulted in decreasing amount of Fe^{2+} ions and consequently, the reaction between Fe^{2+} ions and PS anions prevented according to Eq. (11) [30].

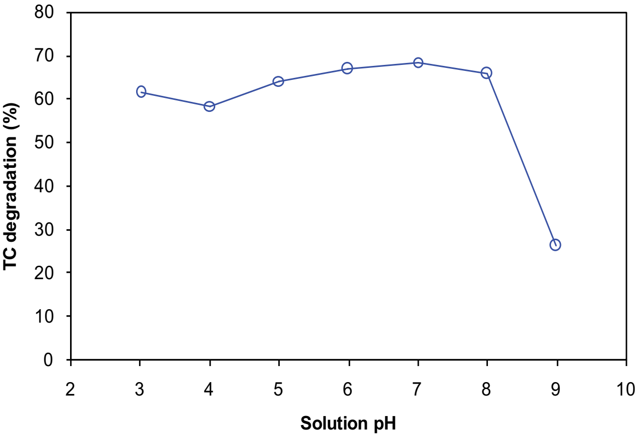

Fig. 1. Effect of solution pH on TC degradation efficiency by PS-EC process (TC concentration: 20 mg/L, PS dose: 100 mg/L, electrolyte concentration: 1 g/L, current density: 1.35 mA/cm^2, and reaction time: 30 min).

$$Fe^{2+} + H_2O \longrightarrow FeOH^{+} + H^{+} \tag{11}$$

Also, formation of Fe^{3+} oxyhydroxides such as $FeOH^{2+}$, $Fe(OH)_2^{4+}$, $Fe(OH)^{2+}$, $Fe(OH)_3$ and $Fe(OH)_4^{-}$ illustrates lower performance in PS activation to produce $SO_4^{\bullet-}$ radicals as depicted in Eqs. (12)–(14) [30] as follows:

$$Fe^{3+} + H_2O \longrightarrow FeOH^{2+} + H^{+} \tag{12}$$

$$Fe^{3+} + 2H_2 \longrightarrow Fe(OH)^{2+} + 2H^{+} \tag{13}$$

$$2Fe^{3+} + 2H_2O \longrightarrow Fe\left(OH\right)_2^{4+} + 2H^{+} \tag{14}$$

Besides, the less ability of the catalyst to activate PS anions at high solution pH led to lower amount of $SO_4^{\bullet-}$ radical and finally the degradation efficiency of TC by PS-EC process declined [30]. During PS reactivation by Fe^{2+} ions, changing the solution pH may havc resulted in production of other free radicals such as $^{\bullet}OH$ radicals. Based on the solution pH during process, the $SO_4^{\bullet-}$ radical is the dominant free radicals at solution pH ranging from 3 to 5, both $SO_4^{\bullet-}$ and $^{\bullet}OH$ radicals exist at solution pH of 7–9 (Eq. (15)), and at solution pH higher than 12, only $^{\bullet}OH$ radical is present (Eq. (16)).

$$SO_4^{\bullet-} + H_2O \longrightarrow OH^{\bullet} + H^{+} + SO_4^{2-} \tag{15}$$

$$SO_4^{\bullet-} + OH^{-} \longrightarrow OH^{\bullet} + SO_4^{2-} \tag{16}$$

Furthermore, at basic range, the oxidation potential of $^{\bullet}OH$ radicals is greatly reduced and also it can react with $SO_4^{\bullet-}$ radical (Eq. (17)); thus degradation efficiency of process depleted [40].

$$SO_4^{\bullet-} + OH^{\bullet} \longrightarrow H^{+} + SO_4^{2-} + 0.5O_2 \tag{17}$$

The result obtained in the present study is consistent with Lin et al. [41], who reported that degradation efficiency of acid orange 7 by electro/Fe_3O_4/peroxydisulfate process decreased when solution pH increased from 3 to 9.

3.2. Effect of reaction time

In order to evaluate variation of TC degradation efficiency by PS-EC process as a function of reaction time, a series of experiments were conducted at solution pH of 7, initial TC concentration of 20 mg/L by varying reaction time in the range of 5–90 min and illustrated in Fig. 2.

As can be seen, when the reaction time progress from 5 to 90 min, the degradation efficiency of TC enhanced from 51.3% to 68.5%. The trend of TC degradation was rapid at the beginning and reaching to equilibrium reaction time after 35 min. After this reaction time, the degradation efficiency of TC not significantly improved.

In fact, the reaction time is a critical factor in the pollutants treatment by AOPs [18]. The data obtained in the present study demonstrating that degradation efficiency of TC by PS-EC process highly depends on the reaction time. The operation PS-EC process over equilibrium reaction time led to increased energy consumption, which is not economically favorable due to the overuse of the generated coagulation [42]. According to Faraday's law, with increasing reaction time of EC process, the increasing amount of iron species can limit the elimination efficiency [39]. Farhadi et al. [43] studied the removal of COD from pharmaceutical wastewater and reported after 30 min reaction time, the amount of COD decreased from 330 to 311 mg/L and the efficiency increased from 31.9% to 35.9%. In addition, Bazrafshan et al. [44] demonstrated that in the first 15 min, the rapid removal efficiency obtained and finally in 75 min, approximately 92.7% removal occurred.

3.3. Effect of current density

By changing applied current density from 0.67 to 3.39 mA/cm², the effect of applied current density on degradation efficiency of TC by PS-EC process was investigated by using PS dose of 100 mg/L at solution pH 7 and initial TC concentration of 20 mg/L. Fig. 3 illustrates the variation of TC degradation efficiency as a function of applied current density.

As can be observed, when the applied current density increased from 0.67 to 2.71 mA/cm², the TC degradation efficiency enhanced from 64.7% to 81.2%. But, further increasing current density above 2.71 mA/cm² led to depletion of degradation efficiency of TC and reaching to 76.5% at current density of 3.39 mA/cm².

In electrochemical oxidation process, the applied current density is the main controlling and anode corrosion occurred by connecting to electricity and led to Fe^{2+} production and generation of $SO_4^{\bullet-}$ radicals according to Eq. (5) [45,46]. The enhancing applied current density led to the rapid iron production and Fe^{2+} regeneration, higher rate of PS decomposition, and finally, improvement of $SO_4^{\bullet-}$ radicals formation by the electron transfer reaction (Eq. (18)).

$$S_2O_8^{2-} + e^- \longrightarrow SO_4^{\bullet-} + SO_4^{2-} \tag{18}$$

On the other hand, increasing the applied current density resulted in the cathodic revival of Fe^{3+} (Eq. (7)) and consequently, higher amount of PS anions got converted to $SO_4^{\bullet-}$ radicals (Eq. (5)) [41,47]. Table 3 summarized the comparison of applied current density in literature.

But, further increasing current density above 2.71 mA/cm² led to depletion of degradation efficiency of TC and reaching to 76.5% at current density of 3.39 mA/cm². The excessive production of Fe^{2+} and their accumulation in solution because of excessive increase of applied current intensity led to scavenging of $SO_4^{\bullet-}$ and $^{\bullet}OH$ radicals by Fe^{2+} ions, which the degradation efficiency of PS-EC process declined, as illustrated in Eq. (21) [46].

$$Fe^{2+} + SO_4^{\bullet-} \longrightarrow SO_4^{2-} + Fe^{3+} \tag{19}$$

3.4. Effect of persulfate dose

To assess the effect of PS dose on PS-EC process, various doses of PS ranging from 100 to 300 mg/L were applied in PS-EC process at solution pH of 7 under 20 mg/L of initial concentration of TC. The variations of TC degradation performance by PS-EC process under different PS dose are displayed in Fig. 4.

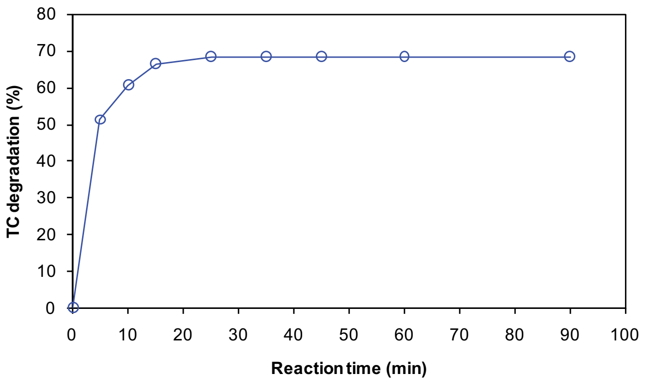

Fig. 2. Influence of reaction time on degradation efficiency of TC by PS-EC process (TC concentration: 20 mg/L, solution pH: 7, PS dose: 100 mg/L, electrolyte concentration: 1 g/L, and current density: 1.35 mA/cm²).

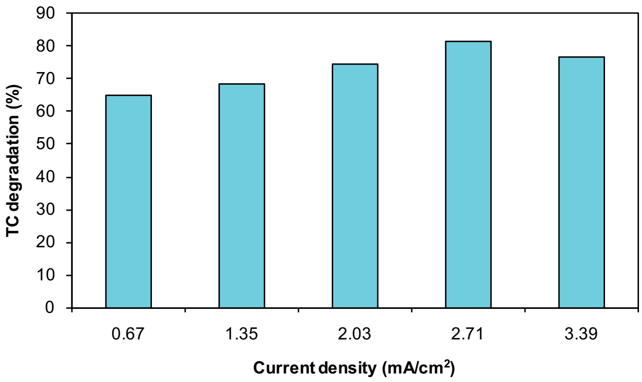

Fig. 3. Effect of applied current density on TC degradation efficiency by PS-EC process (TC concentration: 20 mg/L, solution pH: 7, PS dose: 100 mg/L, electrolyte concentration: 1 g/L, and reaction time: 35 min).

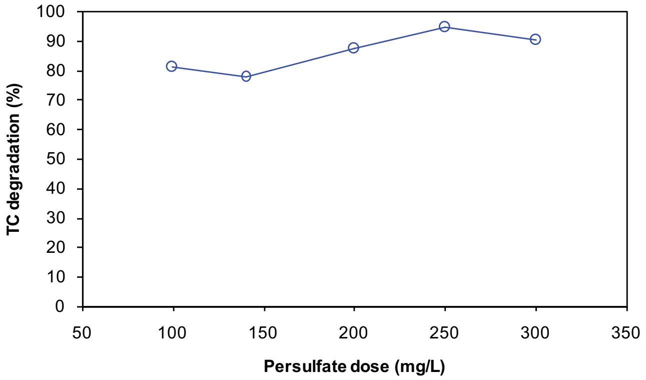

Fig. 4. Variation of TC degradation efficiency by PS-EC process as a function of PS dose (TC concentration: 20 mg/L, solution pH: 7, electrolyte concentration: 1 g/L, current density: 2.71 mA/cm^2, and reaction time: 35 min).

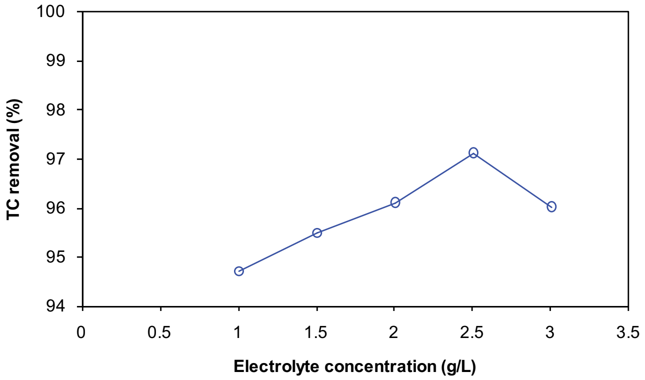

Fig. 5. Influence of concentration of electrolyte on TC degradation efficiency by PS-EC process (TC concentration: 20 mg/L, solution pH: 7, PS dose: 250 mg/L, current density: 2.71 mA/cm^2, and reaction time: 35 min).

As revealed in Fig. 4, with increasing dose of PS from 100 to 250 mg/L, the degradation efficiency of TC by PS-EC process improved from 81.2% to 94.7%. This behavior related to generation of higher amount of $SO_4^{\bullet-}$ radical when higher dose of PS was employed. Variation of removal efficiency as a function of dose of PS is shown in Table 4.

Application of PS dose higher than 250 mg/L led to degradation of TC efficiency decreasing and reached to 90.3% at PS dose of 300 mg/L. When PS dose is very high, the $SO_4^{\bullet-}$ radical may react with surplus PS anions (Eq. (20)), and also with other $SO_4^{\bullet-}$ radicals (Eq. (21)) [50].

$$S_2O_8^{2-} + SO_4^{\bullet-} \longrightarrow SO_4^{2-} + S_2O_8^{\bullet-} \tag{20}$$

$$SO_4^{\bullet-} + SO_4^{\bullet-} \longrightarrow S_2O_8^{2-} \tag{21}$$

Eqs. (20) and (21) resulted in reduction of generation rate of $SO_4^{\bullet-}$ radical and also degradation efficiency of PS-EC process [18,51].

3.5. *Effect of electrolyte concentration*

A series of TC degradation experiments by PS-EC process was carried out to evaluate the effect of electrolyte concentration ranging from 1 to 3 g/L on process performance (Fig. 5).

As expected, the increasing electrolyte concentration has a positive effect on degradation efficiency of TC by PS-EC process. When electrolyte concentration increased from 1 to 2.5 g/L, the degradation efficiency improved from 94.7% to 97.1% and further increasing electrolyte concentration led to degradation efficiency diminishing to 96.15% at 3 g/L of electrolyte concentration. In order to flow the electric current in the electrochemical process, presence of minimal conductivity in the solution is critical, which is obtained by the addition of salts such as NaCl and Na_2SO_4 [52]. The presence of NaCl in optimum concentration in aqueous media led to increasing electrical conductivity, electrical energy reduction, and accelerates the production of hydrogen around the cathode [53]. At a constant current density (or electrical potential), the increasing electrolyte concentration caused electrical conductivity increasing too. Thus, the electric current flows more intensely, which improve Fe^{2+} production and $SO_4^{\bullet-}$ radicals generation and, ultimately, resulting in enhanced degradation efficiency [54]. In addition, increasing the concentration of NaCl can reduce the side effects of other anions such as SO_4^{2-} and HCO_3^-. The application of other salts contain Ca^{2+} and Mg^{2+} can cause formation of insulating layer of $CaCO_3$ and $MgSO_4$ on the electrodes surface, which in turn greatly increases the potential between the electrodes and leads to a significant reduction in current efficiency [55]. Furthermore, Cl^- can react with $SO_4^{\bullet-}$ to form $Cl^\bullet$ (Eq. (22)). Also, chlorine radical ($Cl^\bullet$) can react with additional chloride (Cl^-), forming the dichloride radical ($Cl_2^{\bullet-}$) (Eq. (23)). This process can have an inhibitory effect on sulfate radicals and then reduce them and finally reduce the efficiency of the process [56,57].

A21

$$SO_4^{\bullet-} + Cl^- \longrightarrow Cl^\bullet + SO_4^{2-} \tag{22}$$

$$Cl^\bullet + Cl^- \longrightarrow Cl_2^\bullet \tag{23}$$

Table 3
Results of previous studies along with the present study

Pollutant	Processes	Current density (mA/cm^2)	Increase efficiency%	Refs.
Acid orange 7	Electro/Fe_3O_4/PDS	3.4–25.2	80.3–100	[41]
Tetracycline hydrochloride	Electro-persulfate	6.67–13.3	47.5–81.1	[48]
Clofibric	Electro/Fe^{3+}/PMS	8.4–33.6	40.1–22.6	[49]
Triclosan	PS-EC	0.67–2.71	64.7–81.2	Current study

In the study of Ghalwa et al. [54], during the removal of Abamectin pesticide by electrocoagulation process with iron electrodes, with increasing electrolyte concentration, the efficiency increased and the amount of electrolyte of 1 g/L was selected as optimal, and finally with increasing in NaCl concentration >1 g/L removal efficiency decreased.

3.6. Influence of initial TC concentration

To find the variation of degradation efficiency of TC by PS-EC process with changing initial concentration of TC from 20 to 120 mg/L, the experiments were conducted at solution pH of 7 with application of 250 mg/L of PS and 2.5 g/L of electrolyte and displayed in Fig. 6.

As can be seen, when the initial TC concentration increased from 20 to 120 mg/L, the performance of TC degradation by PS-EC process declined from 97.1% to 48.5%, and similar to reported observation in the literature [2,46].

At constant oxidant content, the increasing concentration of the organic contaminant led to minimizing available oxidation potential and as a result, the performance of AOPs is decreased [54]. In addition, at high concentrations of contaminants, the formation of intermediate compounds in solution may consume oxidizing agents, so the removal efficiency of AOPs is reduced [54,58]. The comparison of previous studies with present study was performed in Table 5.

3.7. Change in the characteristics of the solution

The change in the electrical conductivity (EC) of the solution, temperature, and pH along with the reaction time in the study is shown in Figs. 7a–c.

As illustrated in Fig. 7a, at the beginning of experiment, the value of EC was 4.03 mS/cm, and increased to 5.06 mS/cm after 90 min of reaction time. The EC and ionic resistance of the solution have a great effect on current density efficiency and decreasing ohmic resistance by increasing EC can lead to increasing current density. In addition, the EC can reduce the required reaction, which ultimately leads to a reduction in energy requirement and operating cost [60,61]. Farhadi et al. [43] studied the COD removal from the pharmaceutical wastewater by electrocoagulation process and demonstrated that the EC value decreased from 1,514 to 948 µS/cm after 90 min.

As can be seen from Fig. 7b, at the beginning of the PS-EC process, the pH of the solution was 7 and over reaction time, a gradual increase in pH was observed and reached to 8.27 after 90 min. Farhadi et al. [43] stated that pH control was difficult during the electrocoagulation process and the value of solution pH varied from 7 to 8.75 after 90 min reaction.

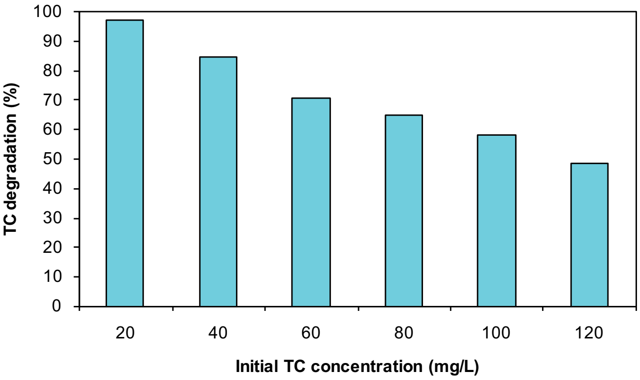

Fig. 6. Trend of TC degradation efficiency by PS-EC process under different TC concentration (solution pH: 7, PS dose: 250 mg/L, electrolyte dose: 2.5 g/L, current density: 2.71 mA/cm^2, and reaction time: 35 min).

In order to find the changes of temperature of the solution during the PS-EC process, the temperature of the solution was measured at different time interval and shown in Fig. 7c. As can be observed, the temperature of the solution gradually increased from 17°C to 29°C. and are in accordance with previously reported data by Farhadi et al. [43], who stated that the temperature increased from 18°C to 27°C during treatment of pharmaceutical wastewater by electrocoagulation process.

4. Operating cost and current efficiency

To evaluate the passivity of the electrodes in terms of the effect on efficiency and energy cost, the current efficiency parameter was investigated. In previous studies, it has been reported that the current efficiency should not be less than 100% and, in this study, the value of this parameter for iron and aluminum electrodes was calculated between 100 to 120 and 100 to 160%, respectively. Calculating the operating cost of various treatment processes is essential to determine its true function in the real world. In this study, the operating cost for triclosan removal from synthetic wastewater was calculated according to the unit price of Iran market (600 Rial/kW of electricity, 225,000 Rial/kg of iron and 535,000 Rial/kg of aluminum). The amount of energy consumed, according to Eq. (9), was 1,166 kWh/m^3. Also, the amount of electrode consumed was

Table 4
Results of previous studies with the present study

Type of pollutant	Processes	PS dose	Increase efficiency%	Refs.
Diclofenac	Electro/Fenton/persulfate	0.25–1.5 mM	49.2–82.1	[50]
Oxcarbazepine	Electro-persulfate	0.1–1 mM	22–83	[23]
Phenol	Electropersulfate	Above 0.5 M	93.99–63.74	[47]
Acid Orange 7	Electro/Fe_3O_4/PDS	10–20 mM	95.8–91.2	[41]
Triclosan	PS-EC	100–250 mg/L	81.2–94.7	Current study

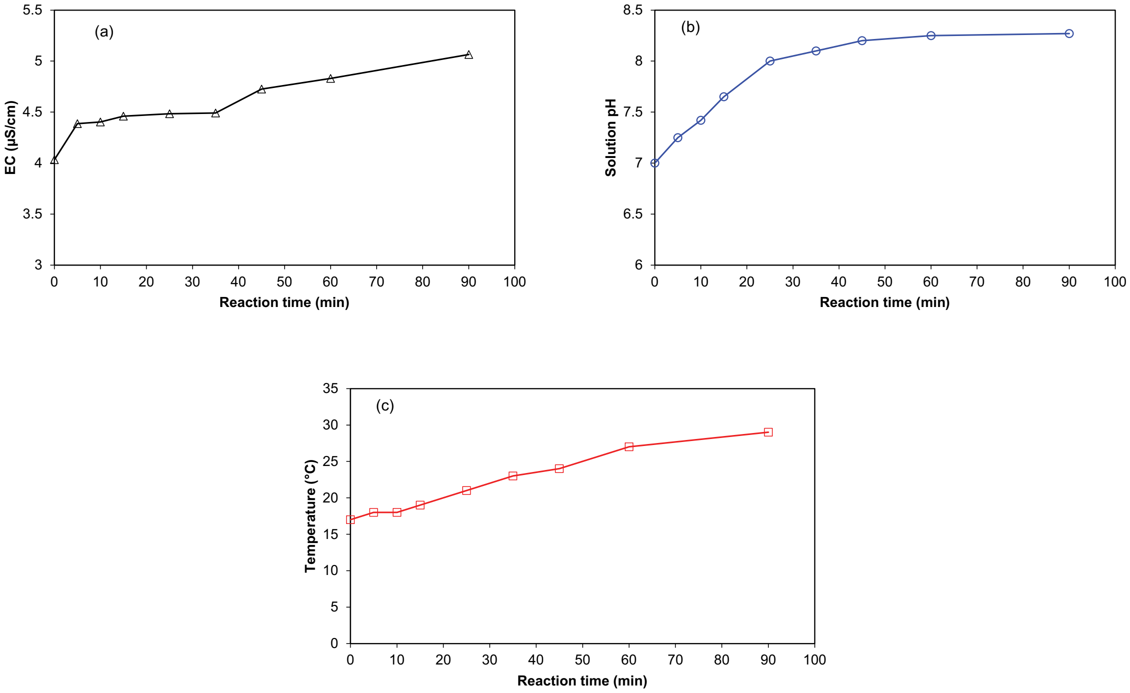

Fig. 7. Variation of EC (a), solution pH (b), and temperature (c) over reaction time during TC degradation by PS-EC process (TC concentration: 20 mg/L, PS dose: 250 mg/L, electrolyte concentration: 2.5 g/L, current density: 2.71 mA/cm²).

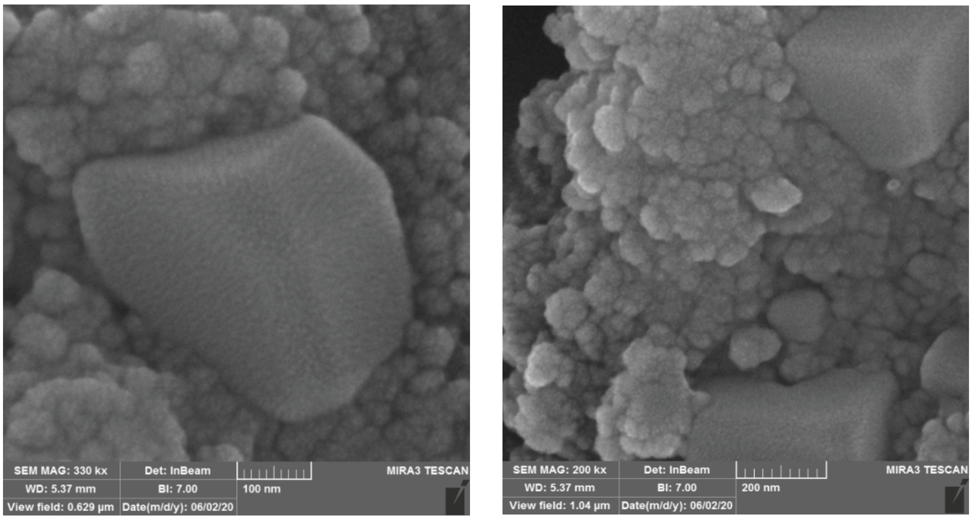

Fig. 8. SEM images of collected sludge during PS-EC process.

calculated using Eq. (10). Then the minimum cost to remove triclosan using the process was studied in this project:

Operating cost = 1,116 kWh/m³ × 600 + 0.4875 kg Fe × (225,000 Rial) + 0.1567 kg AL × (535,000) = 164,782 Rial/m³.

5. Characteristics of the produced sludge

Using SEM observation, the morphology of the settling sludge was determined as shown in Fig. 8.

As can be seen in Fig. 8, the sludge particles have the round shape and lower than 100 nm of size. To provide information about crystalline structures sludge, the XRD analysis was performed and displayed in Fig. 9.

As illustrated in Fig. 9, the distinct and sharp peaks at 2θ = 21.1°, 27.7°, 31.8°, 40.8°, 45.6°, 53.9°, 56.8°, 63.8°, 66.3°, and 75.5° were detected and indicated the presence of sodium chloride (NaCl), sodium sulfate (Na_2SO_4), and disodium persulfide-alpha (Na_2S_2) in collected sludge.

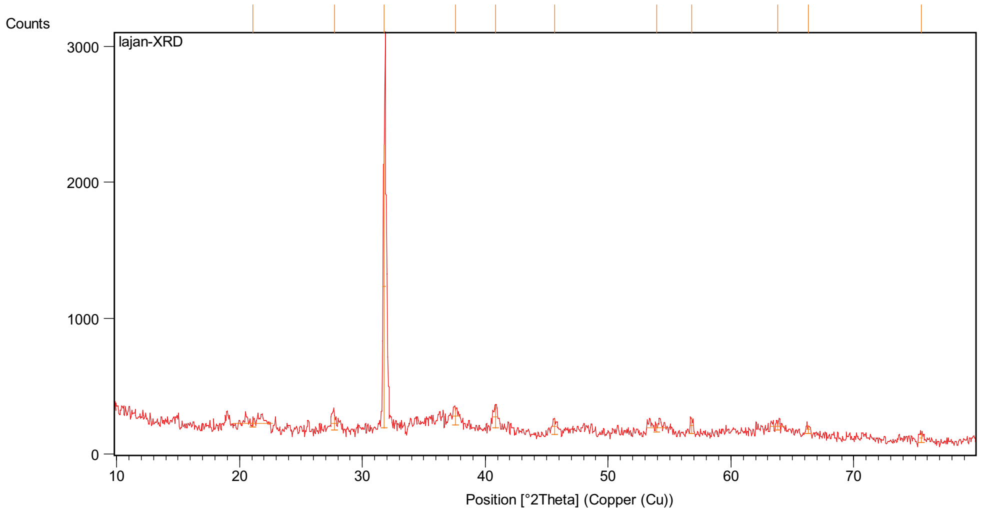

Fig. 9. XRD patterns of collected sludge during PS-EC process.

The functional groups of sludge were determined by FTIR analysis (Fig. 10). The peak at 3,547.9 cm^{-1} and 3,458.6 cm^{-1} may be related to the stretching of the amine N–H bond [62]. The peak at 1,633.1 and 1,469 cm^{-1}, respectively, was attributed to C=C stretching of aromatic rings [63]. 1,469 cm^{-1} can be attributed to phenyl groups and stretching bands of C–O–H. The stretching of Al–O–H and magnetite appeared at 988, 715, and 540 cm^{-1}, respectively [64].

In addition, total pore volume (V_{total}), specific surface area (S_{BET}), and pore size of the collected sludge during PS-EC process were attained from the BET analysis to obtain the values for S_{BET}, V_{total}, average pore diameter as 97.8 m^2/g, 0.19 cm^3/g, and 7.79 nm, respectively.

Because of the presence of different elements in the collected sludge during PS-EC process, the results presented in this study show that the electro-sulfate process, as one of the sulfate-based AOPs, is effective for the degradation of TC in synthetic industrial wastewater. EDX analysis was employed and the pattern of EDX of sludge during PS-EC process using Al-Fe electrodes is shown in Fig. 11.

The EDX spectra of the collected sludge demonstrated that the main elements of sludge are Al (15.9%), Fe (26.1%), Na (2.55%), Cl (2.6%), O (51.1%), and S (1.72%). The presence of Al and Fe in sludge may be related to role of Al and Fe in the EC process and precipitates with the existing contaminants [65]. Irki et al. [66] characterized the flocks formed by the iron-electrocoagulation process and the identified elements are including Al (0.4%), Fe (45.12%), Na (8.9%), Cl (12.54%), O (28.33%), C (4.71%).

6. Conclusion

Today, the overuse of pharmaceuticals and personal care products leads to an increase of these compounds in wastewater and eventually their discharge to surface and

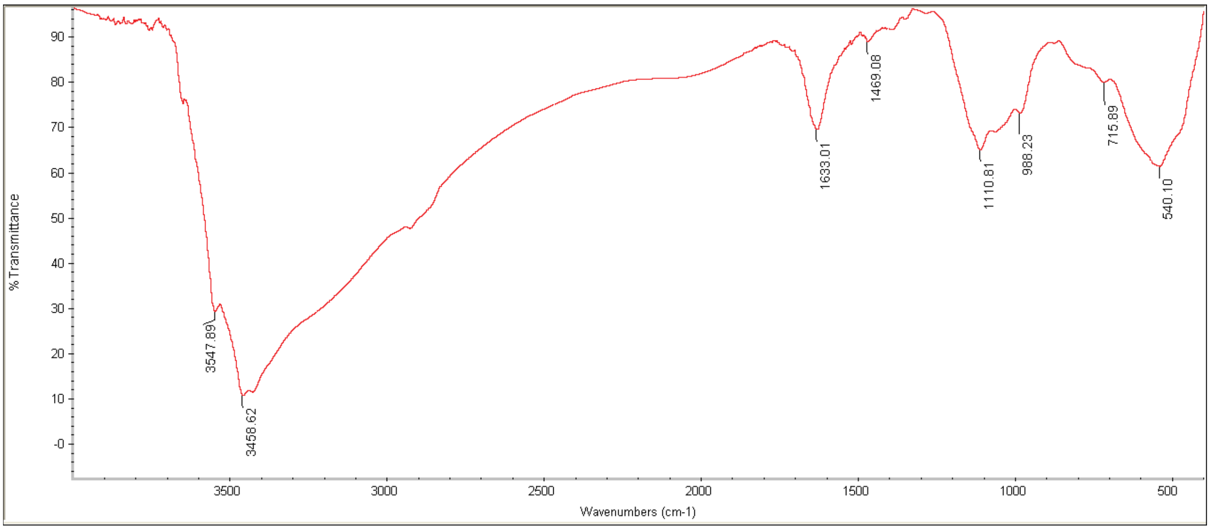

Fig. 10. FTIR spectrum of collected sludge during PS-EC process.

Table 5
Results of previous studies with current results

Type of pollutant	Processes	Concentration of the contaminant	Reduction efficiency (%)	Refs.
Amoxicillin	Electro/Fe_3O_4/Persulfate	15–100 mg/L	92.7–30.9	[46]
Aniline	Fe^{2+}-activated persulfate	10–20 μM	47–42	[59]
Phenol	Electro-persulfate	50–100 mg/L	93.18–15	[47]
Triclosan	PS-EC	20–120 mg/L	97.1–48.4	Current study

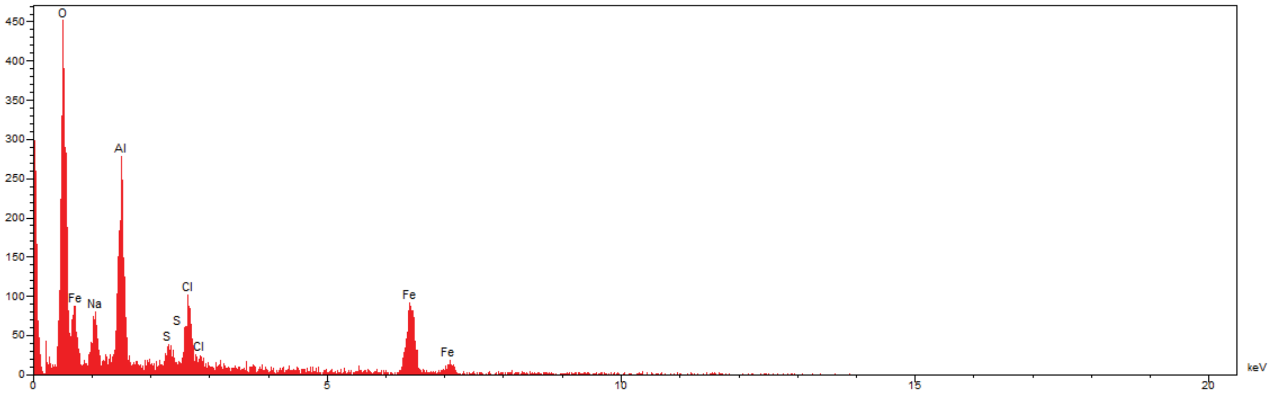

Fig. 11. EDX pattern of the collected sludge during PS-EC process.

groundwater. The purpose of this study was to determine the removal efficiency of TC by the combined PS-EC process using iron electrodes. The TC removal efficiency at different pH in the range between alkaline and acid pH was investigated and the highest removal efficiency was observed at solution pH of 7. As the PS concentration increased, the TC removal rate increased, and with increasing initial TC concentration, the removal efficiency decreased. Increasing the current density to 2.71 mA/cm^2 resulted in improving the removal efficiency of PS-EC process. The generated sludge during PS-EC process was characterized by SEM-EDX, XRD, and FTIR, BET. According to the sharp peaks in the XRD analysis, the sludge contained NaCl, Na_2S_2, Na_2SO_4. The spectra obtained from EDX analysis demonstrated the presence of Al, Fe, Na, Cl, O, and S in the sludge. The results presented in this study show that PS-EC, as one of the sulfate-based AOPs, is effective for the degradation of TC in synthetic industrial wastewater.

Acknowledgments

This study was supported by Shahid Sadoughi University of Medical Sciences (Iran) under Project No. 6173 with the ethics code of IR.SSU.SPH.REC.1398.025. The authors would like to express their gratitude for this support.

References

[1] D. Kriebel, J. Tickner, P. Epstein, J. Lemons, R. Levins, E.L. Loechler, M. Quinn, R. Rudel, T. Schettler, M. Stoto, The precautionary principle in environmental science, Environ. Health Perspect., 109 (2001) 871–876.

[2] S. Wang, J. Wu, X. Lu, W. Xu, Q. Gong, J. Ding, B. Dan, P. Xie, Removal of acetaminophen in the Fe^{2+}/persulfate system: kinetic model and degradation pathways, Chem. Eng. J., 358 (2019) 1091–1100.

[3] A.E. Aiello, E. Larson, Antibacterial cleaning and hygiene products as an emerging risk factor for antibiotic resistance in the community, Lancet Infect. Dis., 3 (2003) 501–506.

[4] R. Chuanchuen, K. Beinlich, T.T. Hoang, A. Becher, R.R. Karkhoff-Schweizer, H.P. Schweizer, Cross-resistance between triclosan and antibiotics in *Pseudomonas aeruginosa* is mediated by multidrug efflux pumps: exposure of a susceptible mutant strain to triclosan selects nfxB mutants overexpressing MexCD-OprJ, Antimicrob. Agents Chemother., 45 (2001) 428–432.

[5] Y.-M. Kim, K. Murugesan, S. Schmidt, V. Bokare, J.-R. Jeon, E.-J. Kim, Y.-S. Chang, Triclosan susceptibility and co-metabolism–a comparison for three aerobic pollutant-degrading bacteria, Bioresour. Technol., 102 (2011) 2206–2212.

[6] Z. Song, N. Wang, L. Zhu, A. Huang, X. Zhao, H. Tang, Efficient oxidative degradation of triclosan by using an enhanced Fenton-like process, Chem. Eng. J., 198 (2012) 379–387.

[7] H. Singer, S. Müller, C. Tixier, L. Pillonel, Triclosan: occurrence and fate of a widely used biocide in the aquatic environment: field measurements in wastewater treatment plants, surface waters, and lake sediments, Environ. Sci. Technol., 36 (2002) 4998–5004.

[8] F. Tohidi, Z. Cai, Fate and mass balance of triclosan and its degradation products: comparison of three different types of wastewater treatments and aerobic/anaerobic sludge digestion, J. Hazard. Mater., 323 (2017) 329–340.

[9] D.E. Latch, J.L. Packer, B.L. Stender, J. VanOverbeke, W.A. Arnold, K. McNeill, Aqueous photochemistry of triclosan: formation of 2,4-dichlorophenol, 2,8-dichlorodibenzo-p-dioxin, and oligomerization products, Environ. Toxicol. Chem., 24 (2005) 517–525.

[10] C. Liyanapatirana, S.R. Gwaltney, K. Xia, Transformation of triclosan by Fe(III)-saturated montmorillonite, Environ. Sci. Technol., 44 (2010) 668–674.

[11] M.J. Martin de Vidales, C. Sáez, P. Cañizares, M.A. Rodrigo, Removal of triclosan by conductive-diamond electrolysis and sonoelectrolysis, J. Chem. Technol. Biotechnol., 88 (2013) 823–828.

[12] Y. Liu, X. Zhu, F. Qian, S. Zhang, J. Chen, Magnetic activated carbon prepared from rice straw-derived hydrochar for triclosan removal, RSC Adv., 4 (2014) 63620–63626.

[13] T.A. Ternes, J. Stüber, N. Herrmann, D. McDowell, A. Ried, M. Kampmann, B. Teiser, Ozonation: a tool for removal of pharmaceuticals, contrast media and musk fragrances from wastewater?, Water Res., 37 (2003) 1976–1982.

[14] S. Suarez, M.C. Dodd, F. Omil, U. von Gunten, Kinetics of triclosan oxidation by aqueous ozone and consequent loss of antibacterial activity: relevance to municipal wastewater ozonation, Water Res., 41 (2007) 2481–2490.

[15] J. Jiang, S.-Y. Pang, J. Ma, Oxidation of triclosan by permanganate (Mn(VII)): importance of ligands and in situ formed manganese oxides, Environ. Sci. Technol., 43 (2009) 8326–8331.

[16] C. Cai, Z. Zhang, H. Zhang, Electro-assisted heterogeneous activation of persulfate by Fe/SBA-15 for the degradation of Orange II, J. Hazard. Mater., 313 (2016) 209–218.

[17] J.E. Silveira, A.L. Garcia-Costa, T.O. Cardoso, J.A. Zazo, J.A. Casas, Indirect decolorization of azo dye Disperse Blue 3 by electro-activated persulfate, Electrochim. Acta, 258 (2017) 927–932.

[18] J. Li, Y. Ren, L. Lai, B. Lai, Electrolysis assisted persulfate with annular iron sheet as anode for the enhanced degradation of 2, 4-dinitrophenol in aqueous solution, J. Hazard. Mater., 344 (2018) 778–787.

[19] B.-T. Zhang, Y. Zhang, Y. Teng, M. Fan, Sulfate radical and its application in decontamination technologies, Crit. Rev. Environ. Sci. Technol., 45 (2015) 1756–1800.

[20] M. Ahmadi, F. Ghanbari, Optimizing COD removal from greywater by photoelectro-persulfate process using Box-Behnken design: assessment of effluent quality and electrical energy consumption, Environ. Sci. Pollut. Res., 23 (2016) 19350–19361.

[21] S. Rodriguez, A. Santos, A. Romero, F. Vicente, Kinetic of oxidation and mineralization of priority and emerging pollutants by activated persulfate, Chem. Eng. J., 213 (2012) 225–234.

[22] Y.-C. Lee, S.-L. Lo, P.-T. Chiueh, D.-G. Chang, Efficient decomposition of perfluorocarboxylic acids in aqueous solution using microwave-induced persulfate, Water Res., 43 (2009) 2811–2816.

[23] L. Bu, S. Zhou, Z. Shi, C. Bi, S. Zhu, N. Gao, Iron electrode as efficient persulfate activator for oxcarbazepine degradation: performance, mechanism, and kinetic modeling, Sep. Purif. Technol., 178 (2017) 66–74.

[24] A. Long, H. Zhang, Selective oxidative degradation of toluene for the recovery of surfactant by an electro/Fe^{2+}/persulfate process, Environ. Sci. Pollut. Res., 22 (2015) 11606–11616.

[25] R.H. Waldemer, P.G. Tratnyek, R.L. Johnson, J.T. Nurmi, Oxidation of chlorinated ethenes by heat-activated persulfate: kinetics and products, Environ. Sci. Technol., 41 (2007) 1010–1015.

[26] M.R. Samarghandi, M. Leili, K. Godini, J. Mehralipour, R. Harati, Furfural removal from synthetic wastewater by persulfate anion activated with electrical current: energy consumption and operating costs optimization, Der Pharma Chem., 7 (2015) 48–57.

[27] F. Ghanbari, M. Moradi, A. Eslami, M.M. Emamjomeh, Electrocoagulation/flotation of textile wastewater with simultaneous application of aluminum and iron as anode, Environ. Process., 1 (2014) 447–457.

[28] O. Sahu, B. Mazumdar, P. Chaudhari, Treatment of wastewater by electrocoagulation: a review, Environ. Sci. Pollut. Res., 21 (2014) 2397–2413.

[29] N. Bektaş, H. Akbulut, H. Inan, A. Dimoglo, Removal of phosphate from aqueous solutions by electro-coagulation, J. Hazard. Mater., 106 (2004) 101–105.

[30] X.-R. Xu, X.-Z. Li, Degradation of azo dye Orange G in aqueous solutions by persulfate with ferrous ion, Sep. Purif. Technol., 72 (2010) 105–111.

[31] E. Bazrafshan, A.H. Mahvi, S. Naseri, A.R. Mesdaghinia, Performance evaluation of electrocoagulation process for removal of chromium(VI) from synthetic chromium solutions using iron and aluminum electrodes, Turk. J. Eng. Environ. Sci., 32 (2008) 59–66.

[32] H. Song, L. Yan, J. Jiang, J. Ma, Z. Zhang, J. Zhang, P. Liu, T. Yang, Electrochemical activation of persulfates at BDD anode: radical or nonradical oxidation?, Water Res., 128 (2018) 393–401.

[33] L. Bu, S. Zhu, S. Zhou, Degradation of atrazine by electrochemically activated persulfate using BDD anode: role of radicals and influencing factors, Chemosphere, 195 (2018) 236–244.

[34] L. Wang, Y. Liu, C. Wang, X. Zhao, G.D. Mahadeva, Y. Wu, J. Ma, F. Zhao, Anoxic biodegradation of triclosan and the removal of its antimicrobial effect in microbial fuel cells, J. Hazard. Mater., 344 (2018) 669–678.

[35] K.S. Hashim, A. Shaw, R. Al Khaddar, M.O. Pedrola, D. Phipps, Iron removal, energy consumption and operating cost of electrocoagulation of drinking water using a new flow column reactor, J. Environ. Manage., 189 (2017) 98–108.

[36] F. Ozyonar, S. Aksoy, Removal of salicylic acid from aqueous solutions using various electrodes and different connection modes by electrocoagulation, Int. J. Electrochem. Sci., 11 (2016) 3680–3696.

[37] A. Rastogi, S.R. Al-Abed, D.D. Dionysiou, Sulfate radical-based ferrous–peroxymonosulfate oxidative system for PCBs degradation in aqueous and sediment systems, Appl. Catal. B, 85 (2009) 171–179.

[38] S. Hammami, N. Oturan, N. Bellakhal, M. Dachraoui, M.A. Oturan, Oxidative degradation of direct orange 61 by electro-Fenton process using a carbon felt electrode: application of the experimental design methodology, J. Electroanal. Chem., 610 (2007) 75–84.

[39] N. Jaafarzadeh, M. Omidinasab, F. Ghanbari, Combined electrocoagulation and UV-based sulfate radical oxidation processes for treatment of pulp and paper wastewater, Process Saf. Environ. Protect., 102 (2016) 462–472.

[40] A. Romero, A. Santos, F. Vicente, C. González, Diuron abatement using activated persulphate: effect of pH, Fe (II) and oxidant dosage, Chem. Eng. J., 162 (2010) 257–265.

[41] H. Lin, H. Zhang, L. Hou, Degradation of CI Acid Orange 7 in aqueous solution by a novel electro/Fe_3O_4/PDS process, J. Hazard. Mater., 276 (2014) 182–191.

[42] K. Godini, G. Azarian, D. Nematollahi, A. Rahmani, H. Zolghadrnasab, Electrochemical treatment of poultry slaughterhouse wastewater using iron and aluminium electrodes, Res. J. Chem. Environ., 16 (2012) 98–103.

[43] S. Farhadi, B. Aminzadeh, A. Torabian, V. Khatibikamal, M.A. Fard, Comparison of COD removal from pharmaceutical wastewater by electrocoagulation, photoelectrocoagulation, peroxi-electrocoagulation and peroxi-photoelectrocoagulation processes, J. Hazard. Mater., 219 (2012) 35–42.

[44] E. Bazrafshan, H. Biglari, A.H. Mahvi, Humic acid removal from aqueous environments by electrocoagulation process using iron electrodes, E-J. Chem., 9 (2012) 2453–2461.

[45] W. Yang, G. Liu, Y. Chen, D. Miao, Q. Wei, H. Li, L. Ma, K. Zhou, L. Liu, Z. Yu, Persulfate enhanced electrochemical oxidation of highly toxic cyanide-containing organic wastewater using boron-doped diamond anode, Chemosphere, 252 (2020) 126499.

[46] F. Sepyani, R.D.C. Soltani, S. Jorfi, H. Godini, M. Safari, Implementation of continuously electro-generated Fe_3O_4 nanoparticles for activation of persulfate to decompose amoxicillin antibiotic in aquatic media: UV254 and ultrasound intensification, J. Environ. Manage., 224 (2018) 315–326.

[47] A.R. Rahmani, H. Rezaeivahidian, M. Almasi, A. Shabanlo, H. Almasi, A comparative study on the removal of phenol from aqueous solutions by electro–Fenton and electro–persulfate

processes using iron electrodes, Res. Chem. Intermed., 42 (2016) 1441–1450.

[48] J. Liu, S. Zhong, Y. Song, B. Wang, F. Zhang, Degradation of tetracycline hydrochloride by electro-activated persulfate oxidation, J. Electroanal. Chem., 809 (2018) 74–79.

[49] H. Lin, J. Wu, H. Zhang, Degradation of clofibric acid in aqueous solution by an EC/Fe^{3+}/PMS process, Chem. Eng. J., 244 (2014) 514–521.

[50] Y. Long, Y. Feng, X. Li, N. Suo, H. Chen, Z. Wang, Y. Yu, Removal of diclofenac by three-dimensional electro-Fenton-persulfate (3D electro-Fenton-PS), Chemosphere, 219 (2019) 1024–1031.

[51] J. Monteagudo, A. Durán, R. González, A. Expósito, In situ chemical oxidation of carbamazepine solutions using persulfate simultaneously activated by heat energy, UV light, Fe^{2+} ions, and H_2O_2, Appl. Catal. B, 176 (2015) 120–129.

[52] M. Keramati, B. Ayati, Petroleum wastewater treatment and optimization of effective parameters using electrocoagulation process, Modares Civil Eng. J., 18 (2019) 177–187.

[53] M. AhmadiMoghadam, H. Amiri, Investigation of TOC removal from industrial wastewaters using electrocoagulation process, Iran. J. Health Environ., 3 (2010) 185–194.

[54] A. Ghalwa, M. Nasser, N. Farhat, Removal of abamectin pesticide by electrocoagulation process using stainless steel and iron electrodes, J. Environ. Anal. Chem., 2 (2015) 134.

[55] G. Chen, Electrochemical technologies in wastewater treatment, Sep. Purif. Technol., 38 (2004) 11–41.

[56] G.-D. Fang, D.D. Dionysiou, Y. Wang, S.R. Al-Abed, D.-M. Zhou, Sulfate radical-based degradation of polychlorinated biphenyls: effects of chloride ion and reaction kinetics, J. Hazard. Mater., 227 (2012) 394–401.

[57] R.S. Magazinovic, B.C. Nicholson, D.E. Mulcahy, D.E. Davey, Bromide levels in natural waters: its relationship to levels of both chloride and total dissolved solids and the implications for water treatment, Chemosphere, 57 (2004) 329–335.

[58] H. Shemer, K.G. Linden, Degradation and by-product formation of diazinon in water during UV and UV/H_2O_2 treatment, J. Hazard. Mater., 136 (2006) 553–559.

[59] Y.Q. Zhang, W.L. Huang, D.E. Fennell, In situ chemical oxidation of aniline by persulfate with iron(II) activation at ambient temperature, Chin. Chem. Lett., 21 (2010) 911–913.

[60] J.N. Hakizimana, B. Gourich, M. Chafi, Y. Stiriba, C. Vial, P. Drogui, J. Naja, Electrocoagulation process in water treatment: a review of electrocoagulation modeling approaches, Desalination, 404 (2017) 1–21.

[61] V. Khandegar, A.K. Saroha, Electrocoagulation for the treatment of textile industry effluent–a review, J. Environ. Manage., 128 (2013) 949–963.

[62] J. de Oliveira Silva, G. Rodrigues Filho, C. da Silva Meireles, S.D. Ribeiro, J.G. Vieira, C.V. da Silva, D.A. Cerqueira, Thermal analysis and FTIR studies of sewage sludge produced in treatment plants. The case of sludge in the city of Uberlândia-MG, Brazil, Thermochim. Acta, 528 (2012) 72–75.

[63] H. Zhao, D. Zhang, P. Du, H. Li, C. Liu, Y. Li, H. Cao, J.C. Crittenden, Q. Huang, A combination of electro-enzymatic catalysis and electrocoagulation for the removal of endocrine disrupting chemicals from water, J. Hazard. Mater., 297 (2015) 269–277.

[64] P. Song, Z. Yang, H. Xu, J. Huang, X. Yang, L. Wang, Investigation of influencing factors and mechanism of antimony and arsenic removal by electrocoagulation using Fe–Al electrodes, Ind. Eng. Chem. Res., 53 (2014) 12911–12919.

[65] M. Nasrullah, L. Singh, S. Krishnan, M. Sakinah, A. Zularisam, Electrode design for electrochemical cell to treat palm oil mill effluent by electrocoagulation process, Environ. Technol. Innov., 9 (2018) 323–341.

[66] S. Irki, D. Ghernaout, M.W. Naceur, A. Alghamdi, M. Aichouni, Decolorizing methyl orange by Fe-electrocoagulation process—a mechanistic insight, Int. J. Environ. Chem., 2 (2018) 18.